ELSEVIER

Available online at www.sciencedirect.com

ScienceDirect

Energy Procedia 55 (2014) 320 – 325

Energy Procedia

4th International Conference on Silicon Photovoltaics, SiliconPV 2014

Boron implanted, laser annealed p^+ emitter for n-type interdigitated back-contact solar cells

Xinbo Yang[a]*, Ralph Müller[b], Avi Shalav[a,c], Lujia Xu[a], Wensheng Liang[a], Rui Zhang[a], Qunyu Bi[a], Klaus Weber[a], Daniel Macdonald[a] and Robert Elliman[c]

[a]*Research School of Engineering, The Australian National University, Canbeera, ACT 0200, Australia*
[b]*Fraunhofer Institute for Solar Energy Systems(ISE), Heidenhofstrasse 2, D-79110 Freiburg, Germany*
[c]*Research School of Physics and Engineering, The Australian National University, Canbeera, ACT 0200, Australia*

Abstract

Ion implantation and laser processing technologies are very attractive for the fabrication of industrially feasible interdigitated back-contact (IBC) solar cells. In this work, p^+ emitters were fabricated by boron implantation and laser annealing, and the electrical properties of emitters were investigated. An emitter sheet resistance (R_{sh}) in the range of 30-200 Ω/□ could be achieved by varying the implanted dose. The saturation current density (J_{oe}) of the passivated p^+ emitter with R_{sh} of ~125 Ω/□ reached 95 fA/cm^2, and the contact resistivity was determined to be as low as 5×10^{-6} Ω·cm^2. Such localized p^+ emitters can be applied to n-type IBC solar cells, which could avoid the high temperature thermal annealing step and related problems.

© 2014 The Authors. Published by Elsevier Ltd. This is an open access article under the CC BY-NC-ND license (http://creativecommons.org/licenses/by-nc-nd/3.0/).
Peer-review under responsibility of the scientific committee of the SiliconPV 2014 conference

Keywords: silicon solar cells; ion implantation; laser annealing; n-type interdigitated back-contact solar cells

1. Introduction

N-type interdigitated back-contact (IBC) solar cells have attracted considerable attention because of their extremely high efficiency. Key advantages associated with the IBC solar cell design involve no optical shading loss with front metal grid (results in high short circuit current density J_{sc}), independent optimization of surface

* Corresponding author. Tel.: +61 02 6197 0112; fax: +61 02 6125 0506.
E-mail address: xinbo.yang@anu.edu.au

1876-6102 © 2014 The Authors. Published by Elsevier Ltd. This is an open access article under the CC BY-NC-ND license (http://creativecommons.org/licenses/by-nc-nd/3.0/).
Peer-review under responsibility of the scientific committee of the SiliconPV 2014 conference
doi:10.1016/j.egypro.2014.08.093

passivation and optics at the front, large metal coverage on the rear that minimizes series resistance, and ease of adopting n-type Si [1]. However, the complex structure and high fabrication cost, which typically required two or more high temperature diffusion and photolithography patterning steps, have limited their commercial mass production.

Recently, interest in ion implantation has been resurrected because of its potential to produce high-efficiency advanced cell structures with fewer processing steps [2, 3]. Up till now, high efficiency p- and n-type solar cells with boron or phosphorus implanted emitters have been reported, and the implanted dopants were activated by high temperature thermal annealing [2-7]. Similarly, patterned ion implantation has been used to fabricate solar cells with selective emitter [8]. As for IBC solar cells, it would be very attractive to use patterned ion implantation to form the interdigitated p^+ and n^+ regions at the rear, which could reduce or avoid high temperature diffusion steps and related problems. However, it is difficult to anneal the phosphorus and boron implanted areas with the same recipe in a single step. Compared to n^+ regions formed by phosphorus implantation and thermal annealing, boron implanted p^+ regions are challenging due to the formation of dislocation loops, incomplete activation, formation of boron rich layers, and the solubility limits in silicon during the thermal annealing [2, 4]. Therefore, thermal annealing of boron implanted regions require a higher temperature (>1000°C) and longer time. Recently, high quality boron-implanted p^+ emitters have been obtained by annealing at 1050°C in a non-oxidizing atmosphere [9]. However, there are numerous disadvantages associated with high temperature annealing steps including: increased processing time; high costs; degradation in bulk lifetime.

Laser annealing has been developed as a more effective way for processing ion implanted silicon [10, 11]. The main advantage is the localised nature of the laser beam, which allows locally melting and doping of the surface area without heating the bulk. Experimental results indicated that laser annealing is superior to thermal annealing as a method for processing ion-implanted silicon, and the lattice damage can be removed much more efficiently with laser annealing [11]. If the boron-implanted p^+ region is locally annealed by the laser, and then the phosphorus implanted n^+ regions could be annealed at a lower temperature, or also annealed by the laser, the high temperature steps can be reduced or even avoided, and the fabrication of n-type IBC solar cells could be simplified significantly. In this work, localized p^+ emitters were fabricated by boron implantation and laser annealing, and the quality of the emitter annealed with different laser fluences was investigated by the QSSPC technique.

2. Experimental procedures

Symmetrical lifetime test samples for QSSPC measurements were prepared on 100 Ω·cm n-type wafers. After an RCA clean, boron was implanted on both sides with a dose between 5×10^{14} and 5×10^{15} cm^{-2} with a low energy of 5kV at Fraunhofer ISE (Varian VIISta HC). The samples were RCA cleaned again before laser annealing. A pulsed KrF excimer laser (248 nm) was used for the annealing. A 32×32 mm^2 area was annealed with different laser fluences on quartered wafers. All the samples were RCA cleaned again and then passivated by plasma enhanced atomic layer deposition (PE-ALD) Al_2O_3 (20nm) followed by a forming gas anneal at 400°C for 30 mins. The emitter sheet resistance (R_{sh}) was measured by a four point probe and the dopant profile was measured by the electrochemical capacitance-voltage (ECV) profiling. The effective lifetime (τ_{eff}), implied V_{oc} (i-V_{oc}) and emitter saturation current density (J_{oe}) were obtained by the QSSPC technique. The transfer length method (TLM) was used to determine the contact resistivity (ρ_c) of the p^+ emitters. Aluminium (~1 µm) was evaporated on the emitter, and a TLM pattern was defined using photolithography. Current-voltage measurement was done on a Keithley 2425 Source Meter. ρ_c was obtained from an extrapolation of resistance versus pad spacing.

3. Results and discussion

Fig.1 shows the minimum R_{sh} that can be obtained with different implanted boron doses. With increasing implant dose, the minimum R_{sh} decreases and a higher laser fluence is required to reach the R_{sh}. The R_{sh} can be adjusted in the range of 30-215 Ω/□ by varying the doses between 5×10^{14} and 5×10^{15} cm^{-2}. Doses between 8×10^{14} and 2×10^{15} cm^{-2} corresponding to R_{sh} values between 65 and 150 Ω/□, as indicated by the red box, are likely to be most useful for solar cell fabrication since for. For high efficiency n-type IBC solar cells, the p^+ emitter often has an R_{sh} of 100-

120 Ω/□ [1]. Therefore, this work will focus on the annealing of boron implanted samples with an implantation dose of 1e15, which resulted in an R_{sh} of ~125 Ω/□.

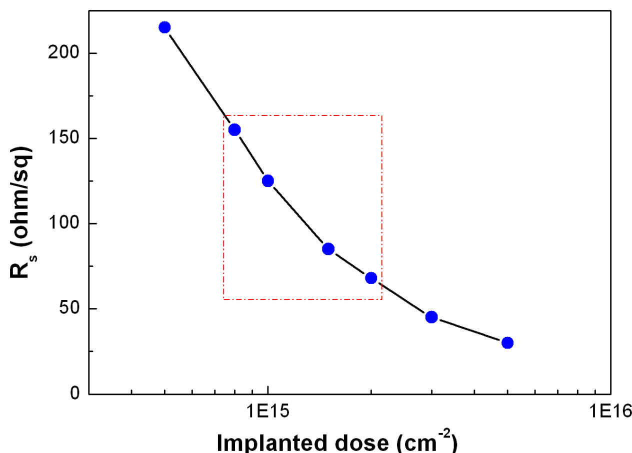

Fig.1. The minimum R_{sh} obtained by laser annealing with different implanted boron doses.

Fig. 2 shows the variation of R_{sh} and τ_{eff} of the samples implanted with the dose of 5×10^{15} cm^{-2} as a function of the laser fluence. R_{sh} decreases with increasing laser fluences, and a minimum R_{sh} of ~125 Ω/□ is reached in the fluence range between 3.5 to 4.0 J/cm^2. For higher fluences, R_{sh} increases, most likely attributed to the increasing evaporation of molten silicon. The τ_{eff} of the samples (at the injection level of 1E15 cm^{-3}) initially increases as the laser fluence increases. The highest τ_{eff} (585 µs) is obtained with a fluence of 3.46 J/cm^2, and decreases for higher laser fluences. The calibrated PL image of four quarter samples also confirmed the results, as shown in the Fig. 3. The sample annealed with a fluence of 3.46 J/cm^2 shows the highest PL intensity. The area without laser annealing shows a very low PL intensity (almost dark), suggesting the samples have a very low effective lifetime directly after the ion implantation, most likely due to sub-surface damage caused during the implant process. The uniform PL intensity of the laser annealed areas also indicated that as-obtained p^+ emitter shows high doping uniformity. TEM results shows that no damage remains in the laser-annealed specimens in the form of dislocations, stacking faults, or dislocation loops [11]. By contrast, after thermal annealing (1000℃ for 10 min in N_2 ambient), the τ_{eff} is much lower than that of laser annealing [4], and significant damage remains in the form of dislocation loops or B-rich clusters [4, 12]. Therefore, lattice damage can be removed much more efficiently with laser annealing than with thermal annealing at ≤ 1000℃.

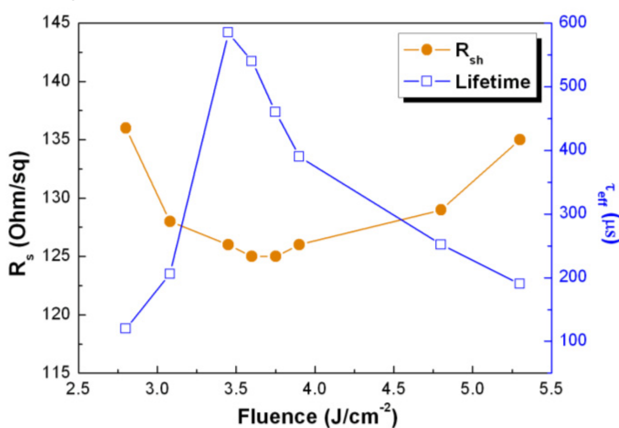

Fig. 2. Variation of R_{sh} and τ_{eff} of the samples as a function of laser fluence.

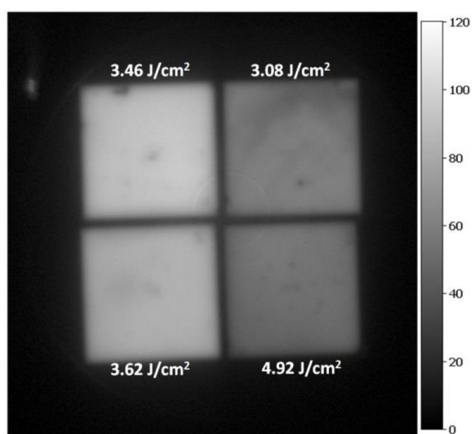

Fig. 3. Calibrated PL image of the implanted samples

annealed with different fluences. The unit is microsecond.

Fig.4 shows the J_{oe} and i-V_{oc} of the passivated samples annealed with different fluences. The J_{oe} values were extracted from the QSSPC measurement using the high injection method. The J_{oe} of the samples decreases as the fluence increases, and a minimum value of 95 fA/cm^2 (extracted at the injection level of 1E16) is obtained with a fluence of 3.46 J/cm^2. A maximum i-V_{oc} of 650 mv is achieved at the same fluence, which is much higher than that obtained via thermal annealing (589 mV) [4]. For higher fluence, the J_{oe} value increases and i-V_{oc} decreases again. The J_{oe} of un-passivated samples show a similar trend, and a minimum J_{oe} value of ~2000 fA/cm^2 can be achieved. After thermal annealing at 1000°C for 20 min, a higher J_{oe} value of ~180 fA/cm^2 was achieved [13]. Dislocation loops or B-rich clusters show stable characteristic even at temperature up to 1000°C [12], giving rise to a drastic increase of SRH recombination rate in the emitter. Until the annealing temperature was increased to 1050°C, a low J_{oe} value of ~34 fA/cm^2 could be obtained, which is close to the calculated theoretical limit of ~20 fA/cm^2 [9]. The results indicate that the implantation damage can only be sufficiently removed when annealed at a high temperature of 1050°C. The relative high J_{oe} value for the laser annealed emitter mainly could be attributed to high boron surface concentration (shown in Fig. 5). Moreover, the laser induced defects (mainly point defects) during the high speed recrystallization [14] may also increase the J_{oe}, which could be improved by heating the substrate during the annealing [15].

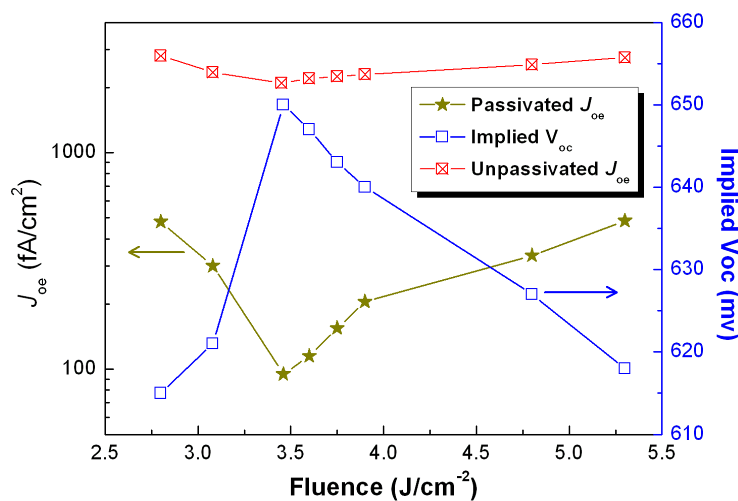

Fig. 4. The J_{oe} and implied V_{oc} of the passivated samples annealed with different fluences. The J_{oe} of unpassivated samples is also shown.

Fig. 5 shows the ECV dopant profile of boron implanted (1×10^{15} cm^{-2}) samples annealed with different laser fluences. As the laser fluence increases, the surface concentration decreases and the junction depth increases. Compared with the diffused emitters, a relative high surface concentration and shallow junction depth is observed for as-obtained emitters. For the sample annealed with the optimized fluence of 3.46 J/cm^2, the surface concentration (7.7×10^{19} cm^{-3}) is higher and junction depth (~0.25 µm) is smaller than that of corresponding thermal annealed samples (surface concentration ~3×10^{19} cm^{-3}, junction depth ~0.60 µm) [9], which is shown together in Fig.5. The different dopant profiles can be attributed to the different annealing mechanisms. Laser annealing involves melting of the Si crystal in the near-surface region, dopant diffusion in the molten state, and, subsequently, liquid phase epitaxial regrowth from the underlying substrate. Implanted dopants will occupy substitutional sites in the silicon lattice after annealing, even when the dopant concentration far exceeds the limits of equilibrium solid solubility [11], which is support by the fact that all the implanted boron is active for the laser annealed samples. Usually, the junction depth is somewhat shallower than the melt depth. However, thermal annealing relies heavily on the solid phase epitaxial regrowth of the damaged near-surface region and activation of the implanted ions. This can lead to more defective material due to the propagation of defects from the amorphous/crystallize interface. Müller *et al.*'s work also proved that for dose higher than 3×10^{15} cm^{-2}, the implanted boron can't be fully activated

at 1050℃ [9]. Usually, ρ_c could benefit from a high surface concentration. According to the TLM results, an average low ρ_c of ~ 5×10^{-6} Ω cm^2 with evaporated aluminium is achieved, indicating a good electrical contact of aluminium to the boron implanted, laser annealed p^+ emitter.

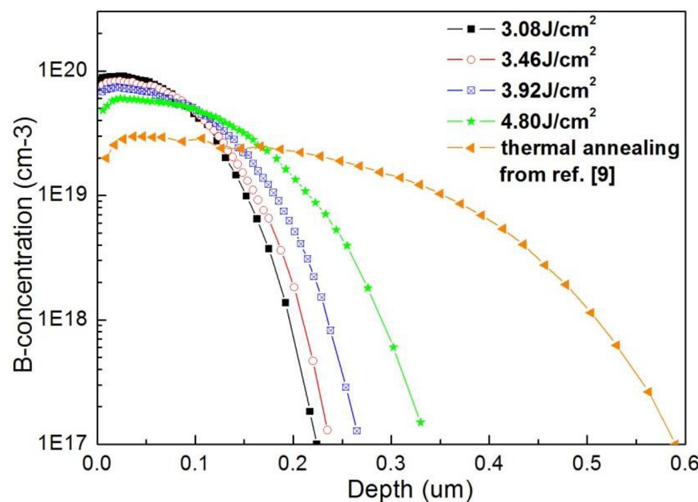

Fig. 5. ECV profile of boron implanted samples annealed with different laser fluences. The SIMS profile of thermally annealed boron implanted emitter from Ref. [9] is shown for comparison.

4. Conclusions

The properties of boron implanted, laser annealed p^+ emitters for n-type IBC solar cells have been investigated and compared with those achieved via thermal annealing. As-obtained p^+ emitters show a high surface boron concentration, shallow junction depth, a low J_{oe} of 95 fA/cm^2, and an average ρ_c of 5×10^{-6} Ω cm^2 with evaporated aluminium can be achieved on the emitter with R_{sh} of ~125 Ω/□. The results indicate that localized laser annealing provides an efficient way to anneal boron implanted p^+ emitters. With both laser and ion implantation technologies (laser annealing and laser contact opening and separation, and patterned ion implantation), high efficiency n-type IBC solar cells should be able to be fabricated without any costly and/or time consuming high temperature (diffusions or annealing) and photolithography (patterning) processing. A simplified and low cost fabrication technology for high efficiency n-type IBC solar cells could therefore be developed. However, the electrical properties of boron implanted, laser annealed p^+ emitters have to be improved in the future.

Acknowledgements

The authors acknowledge financial support from the Australian Solar Institute (ASI)/Australian Renewable Energy Agency (ARENA) under the ANU PV Core project, Postdoctoral Fellowship and Australia-Germany Collaborative Solar Research and Development projects.

References

[1] Zin N, Blakers A, McIntosh KR, Franklin E, Kho T, Chern K, Wong J, Mueller T, Aberle AG, Yang Y, Zhang XL, Feng ZQ, Huang Q, Verlinden PJ. Continued Development of All-Back-Contact Silicon Wafer Solar Cells at ANU. Energy Procedia 2012; 33: 50-63.

[2] Rohatgi, A, Meier DL, McPherson B, OK YW, Upadhyaya AD, Lai JH, Zimbardi F. High-Throughput Ion-Implantation for Low-Cost High-Efficiency Silicon Solar Cells. Energy Procedia 2012; 15: 10-19.

[3] Hermle M, Benick J, Rüdiger M, Bateman N, Glunz SW. N-type silicon solar cells with implanted emitter. 26th European Photovoltaic Solar Energy Conference, 2011; 875-78.
[4] Pawlak BJ, Janssens T, Singh S, Kuzma-Filipek I, Robbelein J, Posthuma NE, Poortmans J, Cristiano F, Bazizi EM. Studies of implanted boron emitters for solar cell applications. Progress in Photovoltaics: Research and Applications 2012; **20**: 106-110.
[5] Kang MG, Lee JH, Boo H, Tark SJ, Hwang HC, Hwang WJ, Kang HO, Kim D. Effects of annealing on ion-implanted Si for interdigitated back contact solar cell. Current Applied Physics, 2012; 12: 1615-18.
[6] Hieslmair H, Mandrell L, Latchford I, Chun M, Sullivan J, Adibi B. High Throughput Ion-Implantation for Silicon Solar Cells. Energy Procedia 2012; 27: 122-128.
[7] Lanterne A, Gall S, Manuel S, Monna R, Ramappa D, Yuan M, Rivalin P, Tauzin A. Annealing, Passivation and Contacting of Ion Implanted Phosphorus Emitter Solar Cells. Energy Procedia 2012; 27: 580-85.
[8] Dubé CE, Tsefrekas B, Buzby D, Tavares R, Zhang WM, Gupta A, Low RJ, Skinner W, Mullin J, High efficiency selective emitter cells using patterned ion implantation. Energy Procedia 2011; 8: 706-711.
[9] Müller R, Benick J, Bateman N, Schön J, Reichel C, Richter MA, Glunz SW. Evaluation of implantation annealing for highly-doped selective boron emitter ssuitable for screen-printed contacts. Solar Energy Materials & Solar Cells 2014; 120:431-435.
[10] Young RT, White CW, Clark GJ, Narayan J, Christie WH, Murakami M, King PW, Kramer SD. Laser Annealing of Boron-Implanted Silicon. Applied Physics Letters 1978; **32**: 139-141.
[11] White CW, Narayan J, Young RT. Laser Annealing of Ion-Implanted Semiconductors. Science 1979; 204: 461-468.
[12] Florakis A, Janssens T, Rosseel E, Douhard B, Delmotte J, Cornagliotti E, Poortmans J, Vandervorst W. Simulation of the anneal of ion implanted boron emitters and the impact on the saturation current density. Energy Procedia 2012; 27: 240-246.
[13] Liang P, Han PD, Fan YJ, Xing YP. Annealing studies of boron implanted emitters for n-silicon solar cells. Semicond. Sci. Technol. 2014; 29: 035011
[14] Hameiri Z, Puzzer T, Mai L, Sproul AB, Wenham SR. Laser induced defects in laser doped solar cells. Progress in Photovoltaics: Research and Applications 2011; 19: 391-405.
[15] Young RT, Wood RF, Christie WH, Jellison GE. Substrate Heating and Emitter Dopant Effects in Laser-Annealed Solar-Cells. Applied Physics Letters, 1981; 39: 313-315.